THE JOURNAL OF PHYSICAL CHEMISTRY B

Article

Structurally Related Scaling Behavior in Ionic Systems

S. Cheng, M. Musiał,* Z. Wojnarowska, A. Holt, C. M. Roland, E. Drockenmuller, and M. Paluch*

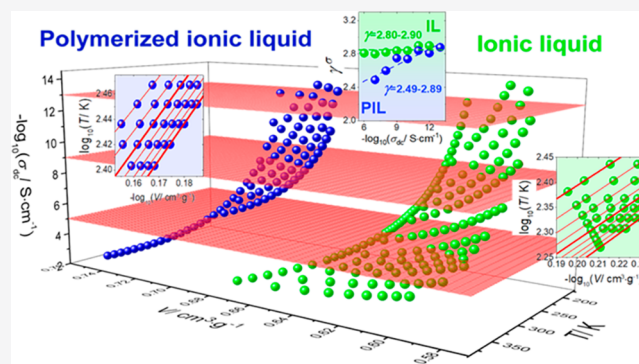Cite This: *J. Phys. Chem. B* 2020, 124, 1240−1244

Read Online

ACCESS | Metrics & More | Article Recommendations | Supporting Information

ABSTRACT: We examine the density scaling properties of two ionic materials, a classic aprotic low molecular weight ionic liquid, 1-butyl-3-methylimidazolium bis(perfluoroethylsulfonyl)imide ([BMIm][BETI]), and a polymeric ionic liquid, poly(3-methyl-1,2,3-triazolium bis(trifluoromethylsulfonyl)imide) (TPIL). Density scaling is known to apply rigorously to simple liquids lacking specific intermolecular associations such as hydrogen bonds. Previous work has found that ionic liquids conform to density scaling over limited ranges of temperature and pressure. In this work, we find that the dc-conductivity of [BMIm][BETI] accurately scales for density changes of 17%; however, there is a departure from scaling for TPIL for even more modest variations of temperature and pressure. The entropy of both ionic samples conforms to density scaling only if the scaling exponent is allowed to vary linearly with the magnitude of the entropy.

INTRODUCTION

There can be little doubt that ionic liquids (ILs) are among the most studied materials of late in the physical sciences. Many theoretical and experimental efforts have been directed toward understanding their complex nature, which is significantly different from that of conventional liquids. Especially of interest are the microscopic details of the structure, the intermolecular forces, and their effect on the relaxation dynamics, charge transport, and the viscoelastic properties. Although electrostatic effects dominate the interactions in ILs, hydrogen bonds, π-stacking of the cation rings, and dispersion forces collectively give rise to diverse and often unique physicochemical behavior, including exceptional chemical stability, low vapor pressures, high enthalpies of vaporization, incombustibility, and high electric conductivity.[1,2] These, in turn, lead to many applications of ILs, e.g., in syntheses, engineering, and electrochemical devices.[2−4]

To design modern electrolytes for next-generation rechargeable batteries the conceptual boundaries of the IL field have expanded to a range of systems characterized by a high density of ions, most notably polymerized ionic liquids (PILs).[5−7] Despite their classification as single-ion conductors, the macromolecular nature of PILs complicates the conductivity behavior.[8] The main mechanism is hopping of nonbonded ions, which is strongly influenced by the size and symmetry of the ions, dissociation energy of the ion pair, the polymer chain flexibility, and the segmental dynamics. These features divide PILs into two groups: materials with charge transport governed by segmental motions and those with ion hopping that is effectively independent of the polymer dynamics. Regardless of the mechanisms underlying ion mobility, suppression of

crystallinity is essential and PILs are very generally good glass-formers.

Exploiting ILs and PILs for technology requires determining their conducting, viscoelastic, and thermodynamic properties over broad conditions of temperature and pressure. This need is magnified by the absence of a generally accepted model to explain and predict the properties, particularly in the vicinity of the melting and glass transition temperatures, T_m and T_g, respectively. One approach to this problem is via density scaling[9,10]

$$x = f(TV^\gamma) \qquad (1)$$

where x represents a physical variable quantifying the molecular dynamics, f is a function, V is the specific volume, T the temperature, and γ the scaling exponent. Equation 1 implies that the viscosity, conductivity, relaxation time, or diffusion constant will superpose onto a single master-curve versus TV^γ.[9,10] The magnitude of the scaling exponent γ is related to the steepness of the repulsive part of the short-range intermolecular potential[11,12] and thus can be treated as a material constant directly related to the structure of the given material. Note it has been shown that the entropy also satisfies the density scaling relation, with a scaling exponent connected to the Gruneisen parameter, γ_G.[13,14] The viscosity of ILs with imidazolium cations and fluorinated anions was shown to
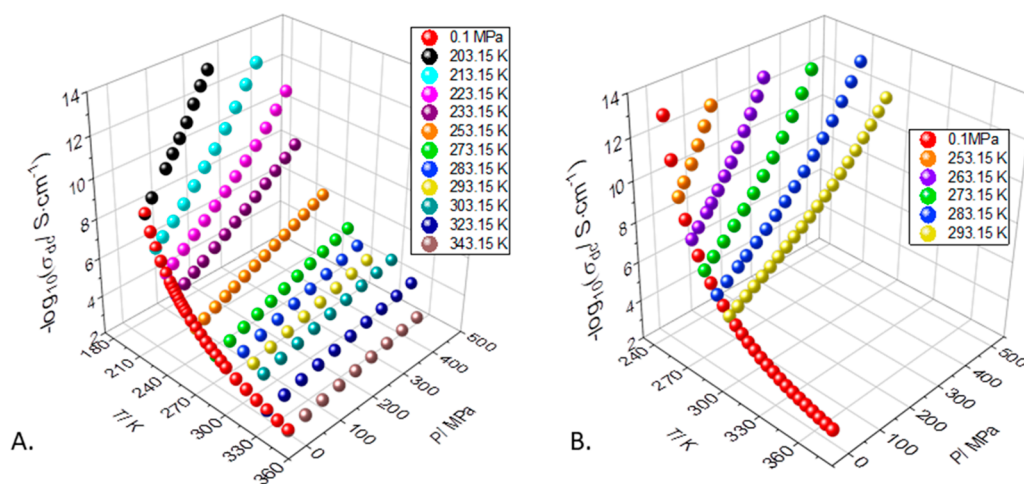
Figure 1. Dc-conductivity, σ_{dc}, data of (A) [BMIm][BETI] and (B) TPIL as a function of temperature and pressure (see the Methods for details).

comply with eq 1.[15] It should be stressed that decoupled ionic liquids with fast proton transport also conform to density scaling.[16−18] If density scaling of the dc-conductivity and entropy can be established generally for both ILs and PILs, it would make possible the prediction of dynamic and thermodynamic properties at any temperature and pressure. This obviously would facilitate the evaluation of new applications and the design of industrial processes employing these materials.

In this work, we investigate the conductivity and entropy for two ionic materials over a broad range of T, P, and V. The materials were a low molecular weight, aprotic IL, 1-butyl-3-methylimidazolium bis(perfluoroethylsulfonyl)imide ([BMIm][BETI]), and a PIL, poly(3-methyl-1,2,3-triazolium bis(trifluoromethylsulfonyl)imide) (TPIL); their structures are shown in Figure S1. Both have potential applications as electrolytes for energy technologies, such as electrochemical devices.

We find that density scaling is accurate for the conductivity of the IL over a broad range of conditions (17% change in V), but data for the PIL show a departure from eq 1. Thus, the scaling exponent for the dc-conductivity, γ^σ, is state-point independent for IL but varies systematically for the PIL, even though for the latter the changes in V were limited to 14%. We also find a relationship between the Gruneisen parameter and the entropy for both materials, from which a single master curve can be constructed, enabling the prediction of thermodynamic properties over all conditions from measurements limited to ambient pressure.

■ METHODS

Materials. **[BMIm][BETI].** 1-Butyl-3-methylimidazolium bis(perfluoroethylsulfonyl)imide (CAS number 254731-29-8; purity >98%) was purchased from Iolitec company (Germany). IL was used without any further purification. Prior to measurements, the sample was dried and degassed under low pressure at temperatures not exceeding 373 K. **TPIL.** A modified protocol was used for the synthesis of TPIL by *N*-alkylation of the 1,2,3-triazole groups and the introduction of the bis(trifluoromethylsulfonyl)imide counter-anions in a single step using *N*-methyl bis(trifluoromethylsulfonyl)imide (CH$_3$TFSI, >90%, Merck) as described earlier.[19] More details can be found in ref 19.

Dielectric Spectroscopy. Dielectric spectra were measured using a Novocontrol Alpha Analyzer, in combination with a Quatro temperature controller with a nitrogen gas cryostat (accuracy better than 0.1 K). Samples were tested in a capacitor arrangement, using steel electrodes (15 mm diameter), with a fixed separation (0.08 mm) maintained by a quartz ring. The applied electric field was 0.1 V.

For measurements at pressures up to 500 MPa, the sample capacitor was placed in a pressure chamber filled with silicone oil. The pressure was measured using a Unipress device with a resolution of 1 MPa. The temperature was controlled within 0.1 K using a Weiss environmental chamber, with measurements as low as 203.2 K.

To parametrize the dc-conductivity data of [BMIm][BETI] the modified Avramov was applied; the details are presented in SI. The dc-conductivities of the TPIL were reported in ref 19.

DSC. Calorimetric experiments of [BMIM][BETI] were performed by a Mettler Toledo DSC1STAR system equipped with a liquid nitrogen cooling accessory and an HSS8 ceramic sensor (a heat flux sensor with 120 thermocouples). The sample was contained in aluminum crucibles with a 40 μL volume. Prior to the measurement, the sample was annealed 15 min at 373 K, followed by heating from 143 to 373 K at rate 10 K min^{-1}. During the experiments, a flow of nitrogen was maintained at 60 mL min^{-1}. Enthalpy and temperature calibrations were performed using indium and zinc standards. Calorimetric experiments of TPIL were reported in ref 19.

TMDSC. Temperature-modulated differential scanning calorimetry measurements were obtained at a heating rate of 0.5 K min^{-1}. The amplitude of the pulses was 1 K.

PVT. **TPIL.** These measurements employed a Gnomix dilatometer,[20,21] with mercury as the confining fluid. The pressure range was 10 to 200 MPa, at temperatures from 303 to 423 K. The accuracy of the obtained specific volume was 0.002 mL g^{-1}. The Gnomix measures only changes in volume; these were converted to absolute values using the specific volume determined for ambient conditions, = 0.7152 mL g^{-1} for TPIL.

[BMIM][BETI]. The mass density of [BMIM][BETI] is well documented in the literature at ambient pressure and different temperatures.[22] The specific volume was measured by a custom-made bellows and piezometer apparatus combined with a Manganin pressure cell from Hardwood Engineering. Hydrostatic pressure was applied to the sample using a manual

Table 1. Coefficients of the EOS Equation (eq 2) along with Standard Deviations

	A_0/mL g^{-1}	$A_1 \times 10^4$/mL g^{-1} K^{-1}	$A_2 \times 10^7$/mL g^{-1} K^{-2}	γ_{EOS}	b_1/MPa	$b_2 \times 10^3$/K^{-1}	δV/mL g^{-1}
[BMIm] [BETI]	0.61698 ± 0.00080	4.02 ± 0.20	1.59 ± 0.11	11.5 ± 0.2	3206.0 ± 6.8	5.1 ± 0.2	0.00002
TPIL	0.69108 ± 0.00011	4.19 ± 0.02	−1.48 ± 0.13	13.1 ± 0.1	3467.7 ± 11.5	4.08 ± 0.03	0.00001

hydraulic pump and intensifier. The pressure range covered was 0.1−400 MPa and with five separate isothermal measurements between 256 and 345 K.

RESULTS

Density Scaling of Conductivity. The dielectric properties of [BMIm][BETI] and TPIL under various thermodynamic conditions were studied by broadband dielectric spectroscopy (see the Methods for details). Representative dielectric spectra of [BMIm][BETI] and TPIL at frequencies from 10^{-1} to 10^7 Hz are presented in the conductivity formalism $\sigma'(f)$ in Figure S2. With shifting along both the ordinate and abscissa, the curves superimpose (inset of Figure S2). From the superposed curves, three regions can be clearly identified for both materials: (i) a low-frequency deviation from the plateau attributed to the polarization effect, typical for ion-conducting materials; (ii) a frequency-independent region associated with the dc-conductivity, σ_{dc}; and (iii) power-law behavior at higher frequencies. The quantity considered in this work is the dc-conductivity, and in both materials σ_{dc} can be detected in the supercooled liquid state as well as at higher temperatures. Thus, the ion dynamics can be followed over 13 orders of magnitude. The σ_{dc} for different isotherms and one isobar at 0.1 MPa are displayed in Figure 1, with the expected decrease with either isobaric cooling and isothermal compression.

More useful for our purposes is the dependence of σ_{dc} on V. PVT results of these materials (specific volume as a function of temperature and pressure is summarized in Table S1; see the Methods for details) were parametrized by fitting an equation of state (EOS) of the form[23]

$$V = \frac{A_0 + A_1(T - T_r) + A_2(T - T_r)^2}{\{1 + (\gamma_{EOS}/b_1)(P - P_r)\exp[b_2(T - T_r)]\}^{1/\gamma_{EOS}}} \quad (2)$$

A_0, A_1, A_2, γ_{EOS}, b_1, and b_2 are material constants, shown in Table 1 with $P_r = 0.1$ MPa and $T_r = T_g = 190.4$ K and $T_r = T_g = 240.8$ K for [BMIm][BETI] and TPIL (obtained from differential scanning calorimetry (DSC); see the Methods), respectively. The choice of T_r at $T_g(P_r)$ is arbitrary; any sufficiently low temperature would suffice.[23] Using the fitted EOS, σ_{dc} is plotted as a function of V (Figure 2A).

As described in the literature, the parameter γ^σ can be determined in different ways.[24−26] In this work we employed the model-independent procedure[26,27] (insets a and b of Figure 2A), according to which $T(V)$ for constant σ_{dc} is plotted double logarithmically versus V, with the slope of the obtained straight line (assuming eq 1 holds) equal to the scaling exponent γ^σ. The average γ^σ values calculated in this way are 2.85 ± 0.05 and 2.69 ± 0.20 for IL and PIL, respectively.

Scaled plots of σ_{dc} versus TV^{γ^σ} are shown in Figure 2C; a collapse of the data onto a single curve is more evident for IL.

Density Scaling of Entropy. To evaluate the dependence of the total entropy on V, S was calculated using
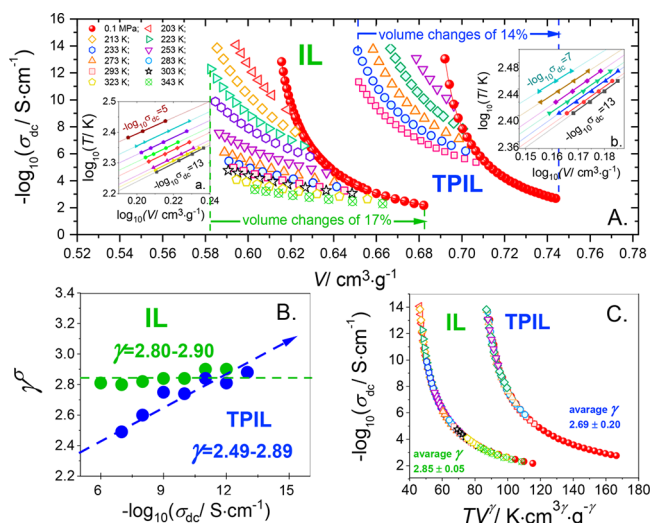
Figure 2. (A) Isothermal and isobaric dc-conductivity data of [BMIm][BETI] and TPIL presented as a function of specific volume. Insets a and b present the results from the horizontal crossing of the $-\log \sigma_{dc}(V)$ data of [BMIm][BETI] and TPIL, respectively. (B) The values of γ^σ for [BMIm][BETI] and TPIL calculated from the slope of the lines presented in insets a and b. (C) Scaled plots of the σ_{dc} data of [BMIm][BETI] and TPIL in terms of TV^{γ^σ}.

$$S(T, P) = S_r(T_r, P_r) + \int_{T_r}^{T} C_P/T \, dT -$$
$$\int_{P_r}^{P} (\partial V(T, P)/\partial T)_P \, dP \quad (3)$$

where S_r is the entropy at the reference condition and the C_P is the molar isobaric heat capacity. C_P is a linear function of T and can be obtained at ambient pressure from temperature modulated differential scanning calorimetry (TM-DSC; see the Methods). The obtained relations were $C_p(T) = 0.7809T + 458.85$ J mol^{-1} K^{-1} for [BMIm][BETI] and $C_p(T) = 14.042T + 24210$ J mol^{-1} K^{-1} for TPIL. Using the PVT data (Table 1), we calculated the third term in eq 3 for different isotherms. This was done for both materials over the same intervals of temperature and pressure ($\Delta T = 140$ K, $\Delta P = 400$ MPa). The results for $S−S_r$ as a function of V are shown in Figure 3A.

To obtain the values of the scaling exponent we employed the method used for the dc-conductivity (insets a and b of Figure 3B), for values of $S−S_r$ from 50 to 300 J mol^{-1} K^{-1} with a step of 50 J mol^{-1} K^{-1} for [BMIm][BETI], and for TPIL, from 1 to 13 kJ mol^{-1} K^{-1} with an increment of 2 kJ mol^{-1} K^{-1}. For both materials, a linear relation is obtained, with a slope yielding the exponent γ_G at constant $S−S_r$, denoted herein γ_G^{S-Sr}. These γ_G^{S-Sr} vary linearly with $S−S_r$ (inset c of Figure 3B). Scaled plots of $S−S_r$ using this nonconstant γ_G^{S-Sr} are shown in Figure 3B.

DISCUSSION

Two ionic materials were studied, a low molecular weight aprotic IL and a macromolecular PIL. The unique feature of the PIL is the pseudo-aromatic structure of the 1,2,3-triazolium
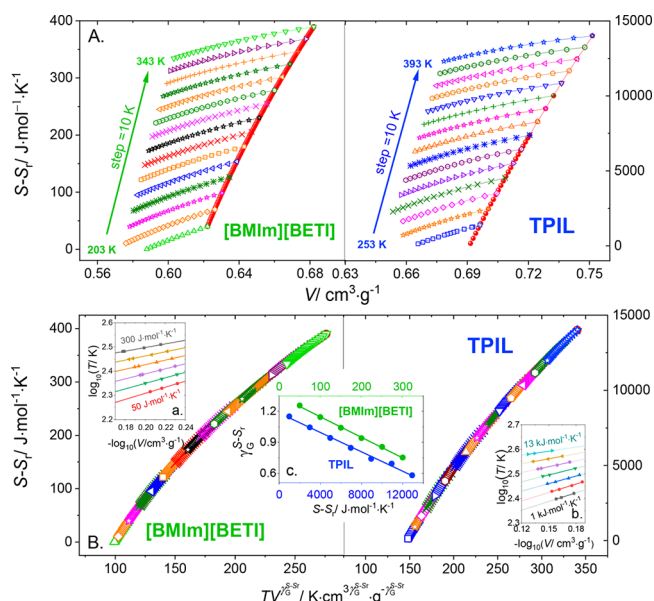
Figure 3. (A) Isothermal and isobaric values of $S-S_r$ of [BMIm]-[BETI] and TPIL plotted as a function of specific volume. (B) A scaled plot of S-S_r of [BMIm][BETI] and TPIL in terms of $TV_{\gamma_G}^{S-S_r}$; that is, the scaling exponent is not constant. Insets a and b the results from the horizontal crossing of the $S-S_r(V)$ data of [BMIm][BETI] and TPIL respectively. Inset c the linear variation of the entropy scaling exponent for [BMIm][BETI] and TPIL calculated from the slope of the lines in insets a and b.

cation along with ethylene oxide in the polymer segment and the bis(trifluoromethylsulfonyl)imide anions with high conformational flexibility, strong delocalization of the negative charge, and an insensitivity to moisture.

Conformance to density scaling of σ_{dc} was assessed for V changes of 17% for the IL and 14% for the PIL (Figure 2A). The obtained scaling exponent for IL is essentially constant (γ^σ = 2.85 ± 2%). This result is at odds with simulations[28] suggesting that density scaling with an invariant exponent is only expected for simple liquids, for example simulated systems interacting via pair potentials having one type of intermolecular repulsive interaction. The expectation is that competition between van der Waals and Coulombic forces would disrupt the correlations, reflected in a breakdown of density scaling. Although electrostatic forces dominate in IL, hydrogen bonding, van der Waals forces, and π-stacking of the cation rings also exert an influence. Nevertheless, the IL tested herein conforms well to density scaling (Figure 2B,C), in agreement with an earlier study of an IL over a more limited range of thermodynamic variables.[15] In the present work, γ^σ remained state-point independent over volume changes of 17%, encompassing the supercooled and high temperature regimes. In contrast, simulations have found departures from eq 1 for similar volume changes.[29]

The PIL offers an interesting contrast because the cations are constrained. The suppression of the cation mobility means the PIL is effectively a single-ion conductor. Nevertheless, for IL and PIL charge transport is strongly coupled to the structural and segmental dynamics, respectively, as shown by the slope of Walden plots (Figure S3) being close to unity. In previous work, based on additional measurements and calculations, it was found that the mobility of ions mimics both the viscosity and segmental relaxation behavior for the

TPIL.[19] More details can be found in ref 19. However, in the case of the PIL, density scaling breaks down, with γ^σ increases by 16% (Figure 2B), over a range that is smaller than for the IL (V changes by 14% vs 17%).

It has been reported previously that the entropy for a number of liquids conforms to density scaling, with the scaling exponent identified with the Gruneisen parameter.[14,30−32] For the IL 1-butyl-3-methylimidazolium bis-(trifluoromethylsulfonyl)imide ([BMIm][TFSI]), density scaling of S was demonstrated over a narrow range, i.e., $\Delta T = 30$ K and $\Delta P = 200$ MPa.[31] However, from the thermodynamic definition of the Gruneisen parameter, $= V\alpha_P C_V^{-1}\kappa_T^{-1}$, where α_P and κ_T are isobaric thermal expansion and isothermal compressibility, respectively, γ_G must change, at least in principle, with changes in temperature and pressure. In this work, we found that, for constant $S-S_r$, γ_G is constant. Thus, the collapse of all data into a single curve cannot be achieved with a constant γ_G (Figure 3).

To summarize, we analyzed density scaling of the dc-conductivity and entropy of two structurally different ionic systems, [BMIm][BETI] and TPIL. For the aprotic IL studied herein, the conductivity data, covering 13 orders of magnitude and volume changes of 17%, collapse onto a single master curve when plotted versus TV^{γ^σ}, with a constant scaling exponent γ^σ. We observe quite different behavior in this first study of a PIL. γ^σ changes by 16% for volume changes of 14%. Concerning scaling of the entropy, for both materials a master curve can be obtained by taking the exponent γ_G^{S-Sr} to be a linear function of S-S_r. In addition to adding to our knowledge base for these important materials, this work demonstrates how their physicochemical properties can be predicted for conditions beyond those measured. This has obvious utility in the design and development of new products and applications.

■ ASSOCIATED CONTENT

Ⓢ Supporting Information

The Supporting Information is available free of charge at https://pubs.acs.org/doi/10.1021/acs.jpcb.9b10783.

Table with specific volume as a function of temperature and pressure for [BMIm][BETI] and TPIL; figures present structures of the tested samples; representative conductivity spectra; Walden plot for [BMIm][BETI] and TPIL; and dc-conductivity of [BMIm][BETI] as a function of temperature and pressure (PDF)

■ AUTHOR INFORMATION

Corresponding Authors

M. Musiał − *Institute of Physics, University of Silesia in Katowice, Silesian Center for Education and Interdisciplinary Research, 41−500 Chorzów, Poland;* ⓞ orcid.org/0000-0002-1624-6617; Email: malgorzata.musial@smcebi.edu.pl

M. Paluch − *Institute of Physics, University of Silesia in Katowice, Silesian Center for Education and Interdisciplinary Research, 41−500 Chorzów, Poland;* ⓞ orcid.org/0000-0002-7280-8557; Email: marian.paluch@us.edu.pl

Authors

S. Cheng − *Institute of Physics, University of Silesia in Katowice, Silesian Center for Education and Interdisciplinary Research, 41−500 Chorzów, Poland;* ⓞ orcid.org/0000-0002-5615-8646

Z. Wojnarowska − *Institute of Physics, University of Silesia in Katowice, Silesian Center for Education and Interdisciplinary Research, 41−500 Chorzów, Poland;* ◉ orcid.org/0000-0002-7790-2999

A. Holt − *Naval Research Laboratory, Chemistry Division, Washington, DC 20375-5342, United States;* ◉ orcid.org/0000-0003-2916-6963

C. M. Roland − *Naval Research Laboratory, Chemistry Division, Washington, DC 20375-5342, United States;* ◉ orcid.org/0000-0001-7619-9202

E. Drockenmuller − *Univ Lyon, Université Lyon 1, CNRS, Ingénierie des Matériaux Polymères, UMR 5223, F-69003 Lyon, France;* ◉ orcid.org/0000-0003-0575-279X

Complete contact information is available at:
https://pubs.acs.org/10.1021/acs.jpcb.9b10783

Notes
The authors declare no competing financial interest.

■ REFERENCES

(1) Fumino, K.; Ludwig, R. Analyzing the interaction energies between cation and anion in ionic liquids: The subtle balance between Coulomb forces and hydrogen bonding. *J. Mol. Liq.* **2014**, *192*, 94−102.

(2) Welton, T. Ionic liquids: a brief history. *Biophys. Rev.* **2018**, *10*, 691−706.

(3) Watanabe, M.; Thomas, M. L.; Zhang, S.; Ueno, K.; Yasuda, T.; Dokko, K. Application of ionic liquids to energy storage and conversion materials and devices. *Chem. Rev.* **2017**, *117*, 7190−7239.

(4) Armand, A.; Endres, F.; MacFarlane, D. R.; Ohno, H.; Scrosati, B. Ionic-liquid materials for the electrochemical challenges of the future. *Nat. Mater.* **2009**, *8*, 621−629.

(5) Wojnarowska, Z.; Feng, H.; Diaz, M.; Ortiz, A.; Ortiz, I.; Knapik-Kowalczuk, J.; Vilas, M.; Verdia, P.; Tojo, E.; Saito, T.; Stacy, E. W.; Kang, N.-G.; Mays, J. W.; Kruk, D.; Wlodarczyk, P.; Sokolov, A. P.; Bocharova, V.; Paluch, M.; et al. Revealing the charge transport mechanism in polymerized ionic liquids: insight from high pressure conductivity studies. *Chem. Mater.* **2017**, *29*, 8082−8092.

(6) MacFarlane, D. R.; Forsyth, M.; Howlett, P. C.; Kar, M.; Passerini, S.; Pringle, J. M.; Ohno, H.; Watanabe, M.; Yan, F.; Zheng, W.; Zhang, S.; Zhang, J. Ionicliquids and their solid-stateanalogues as materials for energygeneration and storage. *Nat. Rev. Mater.* **2016**, *1*, 15005.

(7) Eshetu, G. G.; Mecerreyes, D.; Forsyth, M.; Zhang, H.; Armand, M. Polymeric ionic liquids for lithium-based rechargeable batteries. *Mol. Syst. Des. Eng.* **2019**, *4*, 294−309.

(8) Frenzel, F.; Borchert, P.; Anton, A. M.; Strehmel, V.; Kremer, F. Charge transport and glassy dynamics in polymeric ionic liquids as reflected by their inter- and intramolecular interactions. *Soft Matter* **2019**, *15*, 1605−1618.

(9) Casalini, R.; Roland, C. M. Thermodynamical scaling of the glass transition dynamics. *Phys. Rev. E* **2004**, *69*, 062501−3.

(10) Dreyfus, C.; Le Grand, A.; Gapinski, J.; Steffen, W.; Patkowski, A. Scaling the α-relaxation time of supercooled fragile organic liquids. *Eur. Phys. J. B* **2004**, *42*, 309−319.

(11) Hoover, W. G.; Rossj, M. Statistical theories of melting. *Contemp. Phys.* **1971**, *12*, 339−356.

(12) Coslovich, D.; Roland, C. M. Thermodynamic scaling of diffusion in supercooled Lennard-Jones liquids. *J. Phys. Chem. B* **2008**, *112*, 1329.

(13) Casalini, R.; Mohanty, U.; Roland, C. M. Thermodynamic interpretation of the scaling of the dynamics of supercooled liquids. *J. Chem. Phys.* **2006**, *125*, 014505.

(14) Casalini, R.; Roland, C. M. of supercooled liquids: new results from high pressure data. *Philos. Mag.* **2007**, *87*, 459−467.

(15) Roland, C. M.; Bair, S.; Casalini, R. Thermodynamic scaling of the viscosity of van der Waals, H-bonded, and ionic liquids. *J. Chem. Phys.* **2006**, *125*, 124508.

(16) Wojnarowska, Z.; Tajber, I.; Paluch, M. Density scaling in ionic glass formers controlled by Grotthuss conduction. *J. Phys. Chem. B* **2019**, *123*, 1156−1160.

(17) Swiety-Pospiech, A.; Wojnarowska, Z.; Hensel-Bielowka, S.; Pionteck, J.; Paluch, M. Effect of pressure on decoupling of ionic conductivity from structural relaxation in hydrated protic ionic liquid, lidocaine HCl. *J. Chem. Phys.* **2013**, *138*, 204502.

(18) Swiety-Pospiech, A.; Wojnarowska, Z.; Pionteck, J.; Pawlus, S.; Grzybowski, A.; Hensel-Bielowka, S.; Grzybowska, K.; Szulc, A.; Paluch, M. High pressure study of molecular dynamics of protic ionic liquid lidocaine hydrochloride. *J. Chem. Phys.* **2012**, *136*, 224501.

(19) Cheng, S.; Wojnarowska, Z.; Musiał, M.; Flachard, D.; Drockenmuller, E.; Paluch, M. Access to thermodynamic and viscoelastic properties of poly(ionic liquid)s using high-pressure conductivity measurements. *ACS Macro Lett.* **2019**, *8*, 996−1001.

(20) Fakhreddin, Y. A.; Zoller, P. ANTEC'91. *Society of Plastic Engineers* **1991**, *36*, 1642.

(21) Zoller, P.; Walsh, D. *Standard Pressure−Volume−Temperature Data for Polymers*; Technomic: Lancaster, PA, 1995.

(22) Nazet, A.; Sokolov, S.; Sonnleitner, T.; Makino, T.; Kanakubo, M.; Buchner, R. Densities, viscosities and conductivities of the imidazolium ionic liquids [Emim][Ac], [Emim][FAP], [Bmim]-[BETI], [Bmim][FSI], [Hmim][TFSI], and [Omim][TFSI]. *J. Chem. Eng. Data* **2015**, *60*, 2400−2411.

(23) Grzybowski, A.; Grzybowska, K.; Paluch, M.; Swiety, A.; Koperwas, K. Density scaling in viscous systems near the glass transition. *Phys. Rev. E* **2011**, *83*, 041505−7.

(24) Roland, C. M.; Feldman, J. L.; Casalini, R. Scaling of the local dynamics and the intermolecular potential. *J. Non-Cryst. Solids* **2006**, *352*, 4895−4899.

(25) Roland, C. M.; Casalini, R. Density scaling of the dynamics of vitrifying liquids and its relationship to the dynamic crossover. *J. Non-Cryst. Solids* **2005**, *351*, 2581.

(26) Casalini, R.; Gamache, R. F.; Roland, C. M. Density-scaling and the Prigogine−Defay ratio in liquids. *J. Chem. Phys.* **2011**, *135*, 224501.

(27) Grzybowski, A.; Paluch, M. *Universality of Density Scaling*; Springer: Berlin, 2018.

(28) Bailey, N. P.; Pedersen, U. R.; Gnan, N.; Schrøder, T. B.; Dyre, J. C. Pressure-energy correlations in liquids. I. Results from computer simulations. *J. Chem. Phys.* **2008**, *129*, 184507.

(29) Bøhling, L.; Ingebrigtsen, T. S.; Grzybowski, A.; Paluch, M.; Dyre, J. C.; Schrøder, T. B. Scaling of viscous dynamics in simple liquids: theory, simulation and experiment. *New J. Phys.* **2012**, *14*, 113035.

(30) Roland, C. M.; Casalini, R. EEntropy basis for the thermodynamic scaling of the dynamics of o-terphenyl. *J. Phys.: Condens. Matter* **2007**, *19*, 205118.

(31) Grzybowska, K.; Grzybowski, A.; Pawlus, S.; Pionteck, J.; Paluch, M. Role of entropy in the thermodynamic evolution of the time scale of molecular dynamics near the glass transition. *Phys. Rev. E* **2015**, *91*, 062305.

(32) Masiewicz, E.; Grzybowski, A.; Grzybowska, K.; Pawlus, S.; Pionteck, J.; Paluch, M. Adam-Gibbs model in the density scaling regime and its implications for the configurational entropy scaling. *Sci. Rep.* **2015**, *5*, 13998.